RESEARCH ARTICLE

The pharmacokinetics and pharmacodynamics of cefquinome against *Streptococcus agalactiae* in a murine mastitis model

Qingwen Yang[1], Chenghuan Zhang[2], Xuesong Liu[3,4], Longfei Zhang[5], Kang Yong[1], Qian Lv[1], Yi Zhang[1], Liang Chen[3], Peng Zhong[3,4], Yun Liu[2]*

1 Laboratory of Veterinary Pharmacology, Department of Animal Science and Technology, Chongqing Three Gorges Vocational College, Chongqing, China, 2 Heilongjiang Key Laboratory for Laboratory Animals and Comparative Medicine, Department of Veterinary Surgery, College of Veterinary Medicine, Northeast Agricultural University, Harbin, China, 3 Laboratory of Veterinary Pharmacology, Branch of Animal Husbandry and Veterinary of Heilongjiang Academy of Agricultural Sciences, Qiqihar, China, 4 Heilongjiang Key Laboratory of Veterinary Medicine, Branch of Animal Husbandry and Veterinary of Heilongjiang Academy of Agricultural Sciences, Qiqihar, China, 5 College of Animal Science and Veterinary Medicine, Henan Institute of Science and Technology, Xinxiang, China

* liuyun@neau.edu.cn

Abstract

Cefquinome is a new generation cephalosporin that is effective in the treatment of mastitis in animals. In this study, we evaluated the associations between the specific pharmacokinetics and pharmacodynamics (PK/PD) of cefquinome and its antibacterial activity against *Streptococcus agalactiae* in a mouse model of mastitis. After a single intramammary dose of cefquinome (30, 60, 120, and 240 μg/mammary gland), the concentration of cefquinome in plasma was analysed by liquid chromatography with tandem mass spectrometry (HPLC/MS–MS). The PK parameters were calculated using a one-compartment first-order absorption model. Antibacterial activity was defined as the maximum change in the *S. agalactiae* population after each dose. An inhibitory sigmoid E_{max} model was used to evaluate the relationships between the PK/PD index values and antibacterial effects. The duration for which the concentration of the antibiotic (%T) remained above the minimum inhibitory concentration (MIC) was defined as the optimal PK/PD index for assessing antibacterial activity. The values of %T > MIC to reach $0.5\text{-}log_{10}CFU/MG$, $1\text{-}log_{10}$ CFU/MG and $2\text{-}log_{10}$ CFU/MG reductions were 31, 47, and 81%, respectively. When the PK/PD index %T > MIC of cefquinome was >81% *in vivo*, the density of the *Streptococcus agalactiae* was reduced by $2\text{-}log_{10}$. These findings provide a valuable understanding to optimise the dose regimens of cefquinome in the treatment of *S. agalactiae* infections.

Introduction

Bovine mastitis (BM) is an inflammatory condition of the mammary gland that is caused by trauma or infection and results in the reduced production of both casein proteins and milk

Abbreviations: AUC, The area under the concentration-time curve; MIC, Minimum inhibitory concentration; AUC/MIC, The area under the concentration-time curve to MIC ratio; C_{max}, The peak concentration; C_{max}/MIC, The peak concentration divided by the MIC; MBC, Minimum bactericidal concentration; HPLC, High-performance liquid chromatography; MS, Mass spectrometry; ESI, Electron spray ionisation; PK/PD, Pharmacokinetic/pharmacodynamic; T_{max}, The time to achieve maximum concentration; $T_{1/2e}$, Elimination half-life; %T>MIC, The percentage of concentration that excels MIC.

[1]. BM is a major threat to the dairy industry as it can reduce the quality and volume of milk production. Acute mastitis damages the milk-secreting alveolar cells leading to a permanent reduction in milk yield [2].

Streptococcus agalactiae is a highly contagious obligate pathogenic bacterium found in bovine mammary glands (MGs) [3]. Before the widespread use of antibiotics, it was reported that >85% of BM cases were caused by *S. agalactiae* [4] due to low-grade persistent infections that do not spontaneously resolve. Unidentified infected cows can be reservoirs of infection when they remain untreated or segregated [5]. *S.agalactiae* is a fundamental threat to the dairy industry in many countries [6] and infection is associated with elevated bulk tank somatic cell counts (SCC) and standard plate counts. Economic losses resulting from *S. agalactiae* infections are due to production losses associated with bulk tank SCC, milk quality penalties associated with bulk tank SCC and standard plate counts, and decreases in milk quality associated with bulk tank SCC [7]. The prevalence of *S. agalactiae* in the 4 regions of China ranges between 5.3–17% and is highest in eastern China (17%). The subregional prevalence of *S. agalactiae* ranges between 2.0–25.0% and is highest in the Jiangsu province of eastern China [8]. Between 2017 and 2019, the prevalence of *S. agalactiae* in several regions of the Sichuan province was 33.6% [9]. The detection rate of *S. agalactiae* in Chinese bulk tank milk samples was 92.2% [10].

The widespread misuse of antibiotics has resulted in increased antibiotic resistance leading to treatment failure. Previous studies have shown that in 11 provinces of China, all of the *S. agalgcitae* strains collected from mastitic raw milk samples were multi-resistant to three or more antimicrobial agents [11]. Also, in inner Mongolia, the isolates of *S. agalactiae* from dairy cows with mastitis were found to have a high frequency of β-lactam resistance alone and with tetracyclin or erythromycin [12]. These data highlight the need to optimise the dosing regimens of antibiotics to produce maximum efficacy during treatment.

The pharmacokinetic/pharmacodynamic (PK/PD) integration model is an important method of dosage optimisation, particularly in animal infection models. Only a few studies have used dairy cows as experimental animals because of the management challenges and costs associated with feeding. Other domestic animals, such as goats and sheep, have been used as substitutes yet the cost of these models remains considerable [13]. In comparison, the use of murine models are highly advantageous. A murine mastitis model was first described by Chandler and has since been widely used to study BM [14–16]. Data from murine mastitis models should be interpreted with an appreciation of the differences between the MGs of mice and cows. Several studies have reported on the similarities of bacterial inoculation in the mouse and cow MGs in terms of PMN infiltration and tissue damage [13, 17].

Cefquinome is a newly developed cephalosporin-specific drug that is used in animals [18]. Cefquinome has good PKs and can be absorbed quickly to peak concentrations in the blood [19]. It accumulates at high concentrations in the lungs and MGs, and has low toxicity in animals making it a highly attractive treatment option for various bacterial infections [20, 21]. Compared to systemic therapy, the intramammary administration of cefquinome is more effective in eliminating the causative pathogens of BM [22]. However, no previous studies have investigated the association between the PK/PD indexes and the antibacterial activity of cefquinome in the treatment of *S. agalactiae* infections.

In this study, we used a mouse mastitis model to study the PK/PD integration of cefquinome against *S. agalactiae*. This approach was used to determine the most suitable PK/PD indexe of cefquinome for the treatment of *S. agalactiae* mastitis, and to obtain specific PK/PD index values under different antibacterial conditions.These data provide a valuable understanding of the dose optimisation of cefquinome in the treatment of *S. agalactiae* infections.

Materials and methods

Drugs, bacteria, and animals

Cefquinome sterile powder was obtained from Dr. Ehrenstorfer (lot number G130285; Augsburg, Germany). *S. agalactiae* 3–64 were isolated from dairy cows infected with mastitis. Kunming mice were purchased from the Hunan Silaike Jingda Laboratory Animal (Hunan, China). The mice were maintained in compliance with the American Association for Accreditation of Laboratory Animal Care guidelines [23]. All animal studies were approved by the Laboratory Animal Welfare and Ethics Committee of the Northeast Agricultural University (NEAUEC20191011).

Analysis of minimum inhibitory concentration (MIC), minimum bactericidal concentration (MBC) and mutant prevention concentration (MPC)

MICs were determined by microdilution in compliance with the Clinical Laboratory Standards Institute guidelines [24]. Briefly, colonies were transferred into MHB supplemented with 5% mouse serum and incubated at 37°C on a shaking incubator (220 rpm). The final count was approximately 1×10^8 CFU/mL. 10 μL (1×10^6 CFU/mL) of the culture was used to inoculate each well of a 96-well plate containing broth with different concentrations of cefquinome. A series of two-fold dilutions was achieved by adding 100 μL culture aliquots to a 96-well plate. The MIC was considered the lowest concentration of cefquinome that inhibited bacterial growth in broth after 24 hrs incubation. MBC was determined using a single set of doubling dilutions. The MIC well and four other wells with drug concentrations higher than the MIC were used to establish the MBC using the spot plate count method. The lowest drug concentration that reduced the bacterial count by 99.9% of the original count after 18 hrs was defined as the MBC [25]. Mutant prevention concentrations were determined by applying a high count bacterial suspension (1.5×10^{11} colony-forming units (CFU)/mL) on to an agar plate containing different drug concentrations (1, 2, 4, 8, 16, 32, 64 and 128 multiples of the MIC for each isolate). The concentration ranges were narrowed down. The plates were incubated at 37°C for 72 h and checked for bacterial growth every 24 h. The MPC was defined as the lowest concentration of cefquinome that completely inhibited bacterial growth after 72-hrs [26]. All susceptibility tests were repeated in triplicates.

Establishment of an LC-ESI-MS/MS method for the analysis of cefquinome

The plasma concentrations of Cefquinome were determined by LC-ESI-MS/MS as described previously [27]. Briefly, 100 μl of water containing 0.1% (v/v) formic acid and 100 μL of plasma were combined and vortexed for 3 min. The samples were then centrifuged at $5000 \times g$ for 15 min and the supernatants were harvested. 20 μL of the supernatant was injected into the HPLC system. The limit of detection (LOD) and limit of quantification (LOQ) values for this assay were 0.005 and 0.01 μg/ml, respectively. The recoveries of cefquinome in the plasma samples were >85%. All inter- and intra-assay variations were measured by calculating the relative standard deviation (%RSD) and ensuring that it was <10%.

In vitro killing curve analyses

After 6 hrs of culture, logarithmic phase *S. agalactiae* 3–64 were added to 10 mL of MH broth (5% foetal calf serum) and diluted to 10^6 CFU/mL and 10^7 CFU/mL. A series of concentrations of cefquinome (0×, 0.5×, 1×, 2×, 4×, 8×, and 16× MIC) were added to the bacterial suspensions which were then cultured and incubated at 37°C. The bacterial population was measured at 0,

3, 6, 9, and 12 hrs. After serial 10-fold dilution, samples were plated on to trypticase soy agar (TSA) plates (5% defibrinated sheep blood) and cultured for 18–20 hrs. The detection limit was 300 CFU/mL.

Establishment of a murine mastitis model

A murine mastitis model was established based on previous studies [28, 29]. 8–12 day old pups were removed and lactating mice were anaesthetised with 1% pentobarbital sodium delivered by i.p injection. After 0.15 hrs, the L4 (4th on the left) and R4 (4th on the right) abdominal MGs were disinfected with 75% ethanol and the teat tip was cut using scissors. To prevent environmental bacterial contamination, <1 mm of the tissue was removed. Each teat was held with fine forceps and the duct orifice was located. 100 μL of *S. agalactiae* (5.2×10^5 CFU/mL) was slowly injected through the orifice using a syringe with a blunt needle (<30 gauge).

In vivo antibacterial efficacy

After *S. agalactiae* was injected into the mice, four mice were euthanized by CO_2 asphyxiation and MG samples were collected at 3, 6, 9, 12, 24, 48, and 72 h. MG samples were homogenized and the visible bacterial colonies were counted to establish *in vivo* bacterial growth curves for four experimental groups and one control group. In the mastitis model, a single dose of cefquinome was administered to the MG at a range of concentrations (30, 60, 120, or 240 μg/gland). The control group was treated with saline solution. The limit of detection for the bacteria was 300 CFU/MG.

The pharmacokinetics of cefquinome in murine plasma

PK experiments were performed on lactating Kunming mice. The mice were randomized into four experimental groups (n = 6 each). Sedation and analgesia management were performed as described by Zeng et al. [30]. Briefly, mice were added to an induction chamber (oxygen flow rate = 0.5–1.0 L/min). At the same time, 3%–5% of isoflurane vapour was applied for induction and then reduced to 1%–3% for maintenance. As stated above, after intramammary administration (30, 60, 120, and 240 μg/MG), retro-orbital blood samples (200 μL at each time point) were harvested at 0.083, 0.167, 0.25, 0.5, 0.75, 1, 2, 4, 6, 8, 10, and 12 h after cefquinome administration. The plasma samples were isolated by centrifugation for 10 min ($2500 \times g$, 4°C). The supernatants were stored at -20°C for 2 weeks and the plasma cefquinome concentration was established via HPLC-MS/MS. The linearity of cefquinome quantitation was from 0.01–5 μg/mL and R^2 was >0.99. Cefquinome extraction recovery in the plasma was >80%, and the coefficient of variation was <10% within and between runs. The respective limitations of quantification and detection were 0.01 μg/mL and 0.005 μg/mL. The main PK parameters were harvested using WinNonlin version 5.2.1 (Pharsight, MO, USA). These parameters were the half-life of first-order elimination ($T_{1/2e}$), the half-life of absorption ($T_{1/2\alpha}$), peak plasma concentration (C_{max}), and time of maximum plasma concentration (T_{max}).

PK/PD integration

The PK/PD indexes comprised the AUC/MIC (area under the time-concentration curve divided by MIC), %T > MIC (the percentage time for which the drug concentration exceeded MIC), and C_{max}/MIC (peak concentration divided by MIC). The relationship between *in vivo* antibacterial effects (△log CFU/MG) and the PK/PD indexes were described using an

inhibitory sigmoid E_{max} model [31, 32].

$$E = Emax - \frac{(Emax - E0) \times C_e^N}{EC_{50}^N + C_e^N}$$

where E denotes the antibacterial effect determined based on the maximum change in the bacterial counts ($\log_{10}$ CFU/MG) during 72 h after treatment; E_{max} indicates the maximum change in the bacterial counts in the control group; E_0 represents the maximum change in the bacterial counts in the various experimental groups; EC_{50} is the PK/PD index values that produced antibacterial effects equal to 50% of the maximum; C_e is the PK/PD index; and N is the Hill coefficient, corresponding to the steepness of the effect curve associated with each of the PK/PD indexes.

Statistical analyses

Statistical analyses were conducted by the analysis of variance. Significant differences in the data were analysed using Bonferroni correction and with a P-value threshold of <0.05 set for statistical significance [33].

Results

Chromatogram of cefquinome

The chromatograms for cefquinome in a cefquinome standard solution and the experimental samples are shown in Fig 1. This method had good specificity and was used for the determination of cefquinome.

MIC, MCB and MPC

The MIC of cefquinome against *S. agalactiae* 3–64 was 0.03 μg/mL, the MBC was 0.06 μg/mL, and the MPC was 0.24 μg/mL. For the quality-control ATCC25922 (*Escherichia coli)* and ATCC29213 (*Staphylococcus aureus)* strains, the MIC values were 0.06 and 0.5 μg/mL, respectively.

The PKs of cefquinome in murine plasma

Due to the low protein binding (8%) [34] and precipitation in the samples, we believe that the cefquinome was almost entirely unbound in plasma. The concentration-time data are shown in Table 1. The cefquinome concentration-time curves for the different doses were generated (Fig 2). A one-compartment model with first-order absorption was fitted to calculate the PK parameters (Table 2). The time of the maximum plasma concentration (T_{max}) was 0.20–0.25 hrs (mean, 0.22 hrs). The half-life of first-order elimination ($T_{1/2e}$) was 0.47–0.69 hrs (mean, 0.65 hrs). The peak plasma concentration (C_{max}) increased proportionately with increasing doses of cefquinome along with the area under the time-concentration curve (AUC).

In vitro killing curves

The *in vitro* killing curves are presented in Fig 3 and show that cefquinome is a classical time-dependent drug. The killing rate and bactericidal effects did not increase with an increase in drug concentration. In the low-concentration group ($< 4 \times$ MIC), cefquinome did not have a bactericidal effect. When the concentration reached $>4 \times$ MIC, in the low-concentration-pathogens group, the maximum bactericidal effect achieved a 3-$\log_{10}$ CFU/mL reduction.
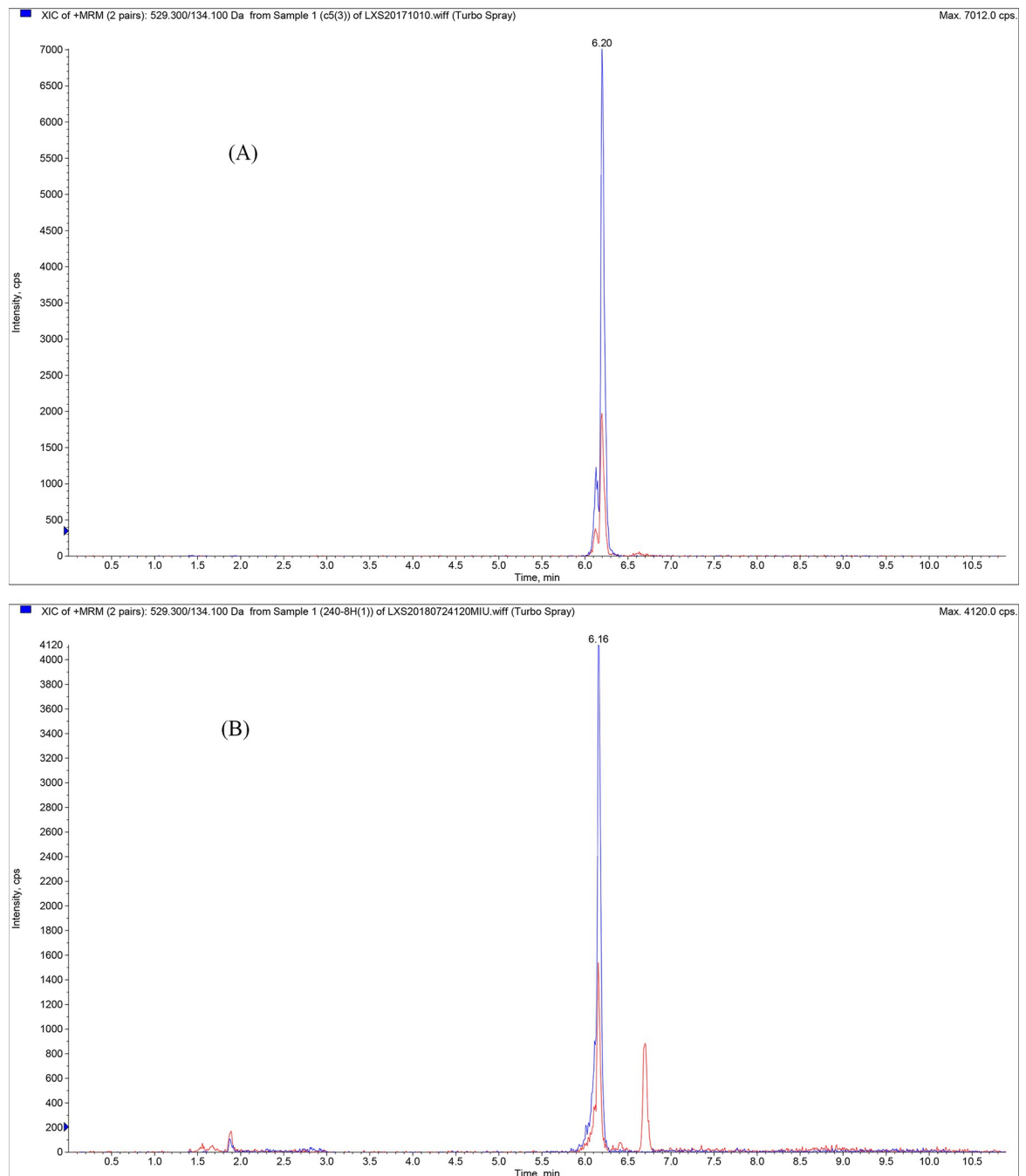
Fig 1. The standard cefquinome and test sample chromatograms. A sample of cefquinome (A) or test sample (B) was analyzed by LC-ESI-MS/MS. For the test sample, cefquinome was extracted as described in the method section and analyzed by LC-ESI-MS/MS (B).

However, in the high-concentration-pathogens group, the maximum bactericidal effect only achieved a 1.2-$\log_{10}$ CFU/mL reduction.

In vivo antibacterial effect

The *in vivo* killing curves are shown in Fig 4. The killing rate of cefquinome in mice was lower than that observed in Mueller–Hinton Broth. However, the killing curve of cefquinome against

Table 1. The cefquinome concentration (µg/mL) in the plasma of mice with *Streptococcus agalactiae*-induced mastitis following intramammary administration of 30, 60, 120, 240 µg/MG.

Time (h)	Does regimen (µg/MG)			
	30	60	120	240
0.083	0.52 ± 0.065	0.825 ± 0.113	2.17 ± 0.217	5.26 ± 0.273
0.167	1.389 ± 0.045	3.93 ± 0.143	4.33 ± 0.282	6.56 ± 0.398
0.25	1.755 ± 0.064	4.39 ± 0.351	7.48 ± 0.553	10.68 ± 0.49
0.5	0.641 ± 0.107	1.21 ± 0.102	3.66 ± 0.222	5.78 ± 0.602
0.75	0.504 ± 0.072	1.007 ± 0.136	1.81 ± 0.104	3.11 ± 0.321
1	0.196 ± 0.029	0.451 ±0.084	1.32 ±0.079	2.22 ± 0.164
2	0.054 ± 0.006	0.176 ± 0.036	0.375 ± 0.039	0.596 ± 0.047
4	0.029 ± 0.006	0.096 ± 0.023	0.143 ± 0.023	0.274 ± 0.043
6	0.019 ± 0.004	0.049 ± 0.01	0.093 ± 0.012	0.131 ± 0.013
8	0.014 ± 0.002	0.03 ± 0.003	0.054 ± 0.006	0.079 ± 0.008
10	0.011 ± 0.002	0.022 ± 0.003	0.038 ± 0.004	0.058 ± 0.006
12	0.009 ± 0.002	0.014 ± 0.002	0.021 ± 0.004	0.036 ± 0.004

https://doi.org/10.1371/journal.pone.0278306.t001

S. agalactiae showed a classical time-dependent pattern. The 30, 60, 120, and 240 µg/MG experimental groups achieved 1.1-$\log_{10}$, 1.2-$\log_{10}$, 2.5-$\log_{10}$, and 2.8-$\log_{10}$CFU/MG reductions, respectively at 72 h. The 120 µg/gland and 240 µg/gland experimental groups almost achieved bactericidal effects but these did not change significantly within increasing drug concentration increased ($P>0.05$).

PK/PD integration and analysis

PK/PD integration of the various PK/PD indexes *versus* the antibacterial effectiveness for the inhibitory sigmoid E_{max} model are shown in Figs 5–7. The R^2 values between the observed PD and predicted PD data of %T > MIC, AUC/MIC, and C_{max}/MIC were 0.9863, 0.9582, and 0.8774, respectively. The key PK/PD parameters are summarized in Table 3. The target values

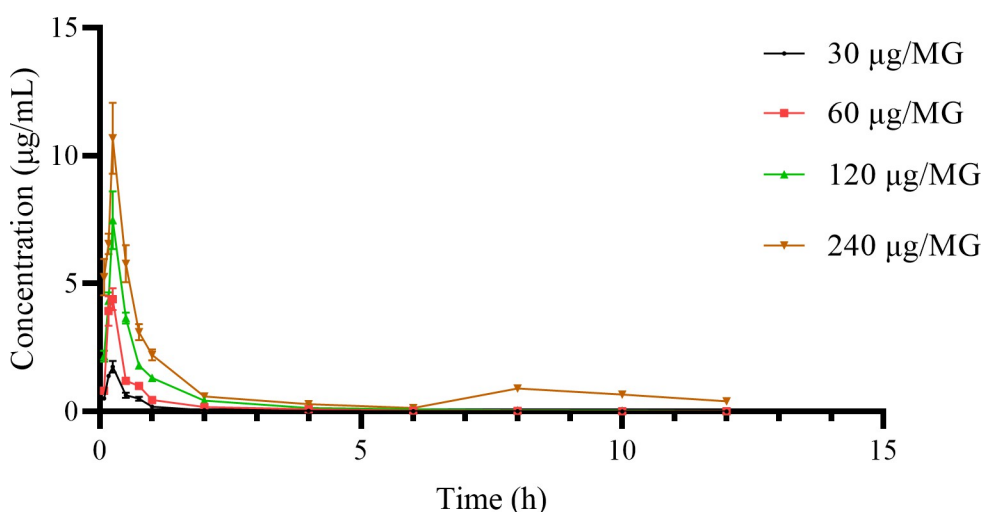**Fig 2. Plot of plasma concentrations of cefquinome versus time in a mouse model of *S. agalactiae* mastitis (n = 6) following a single intramammary administration of 30 µg/MG, 60 µg/MG, 120 µg/MG, and 240 µg/MG.** The bars represent the standard deviations. The cefquinome concentration in plasma was determined by LC-ESI-MS/MS as described in the method section.

https://doi.org/10.1371/journal.pone.0278306.g002

Table 2. The pharmacokinetic parameters of cefquinome in the plasma of mice with *Streptococcus agalactiae*-induced mastitis.

Parameter (units)	Dosage (µg/MG)			
	30	**60**	**120**	**240**
$T1/2_\alpha$ (h)	0.08	0.07	0.07	0.07
$T1/2_e$ (h)	0.61	0.51	0.38	0.46
T_{max} (h)	0.22	0.20	0.25	0.20
AUC (µg.h/mL)	1.16	2.39	5.41	8.33
C_{max} (µg/mL)	1.31	3.20	6.79	8.43
MRT (h)	0.84	0.78	1.06	0.98
Vss (L/kg)	0.22	0.18	0.23	0.28

$T_{1/2\alpha}$ indicates the absorption half-life; $T_{1/2e}$ represents the elimination half-life; T_{max} denotes the time to achieve the maximum concentration; the AUC represents the area under the concentration-time curve; C_{max} indicates the maximum plasma concentration; MRT indicates the mean residence time; Vss represents the volume of distribution.

https://doi.org/10.1371/journal.pone.0278306.t002

of the PK/PD indexes to produce a 0.5-$\log_{10}$ CFU/MG reduction, 1-$\log_{10}$ CFU/MG reduction, and 2-$\log_{10}$ CFU/MG reduction were 31%, 47%, and 81% for %T > MIC; 39 h, 79 h, and 101 h for AUC/MIC; and 43, 98, and 147 for C_{max}/MIC, respectively.

Discussion

In veterinary drug research, PK and PD data are often established in separate parallel studies to formulate the drug delivery scheme which is evaluated and verified in subsequent clinical trials [35]. However, with the widespread use of antibiotics, bacterial resistance has gradually emerged. PK/PD modelling is a vital approach to optimise the use of antibacterial drugs. The elimination half-life (T1/2e) identified in this study (0.49±0.083 hrs) was similar to that previously reported i.e. 0.4 hrs for intramammary administration in an experimental mouse model of *S. aureus* mastitis and 0.43 hrs for the intramuscular injection in the black swan model [27, 36]. However, the value was significantly lower than reported for intramammary administration in lactating Chinese dairy cows (4.63 hrs) which detected the drug concentration in milk and for intramammary administration in an *Escherichiacoli* lactating mouse mastitis model (12.63 hrs) that detected the drug concentration in the MGs [29, 37]. Compared to the cefquinome concentration in MGs, the cefquinome concentration in plasma was much lower which also occurs in cows. This may be related to the chemical properties of cefquinome.

Cefquinome is an organic acid with low fat solubility and pKa values of 2.51 and 2.91 [38]. This causes the distribution of cefquinome to be less extensive and so it cannot penetrate membranes and cross the blood-MG barrier, preventing the drug from reaching the blood from the MG. The $T_{1/2\alpha}$ of 0.07±0.05 hrs was identical to the 0.07 hrs previously reported [36]. In addition to oral administration, the body can rapidly absorb other forms of cefquinome. After metabolism *in vivo*, cefquinome is mainly excreted in the urine through the kidneys [38].

In the present study, after 9 hrs of inoculation in mice MGs, the *S. agalactiae* bacterial burden reached approximately 10^7 CFU/MG. These data showed that the *S. agalactiae*-induced mastitis model could sufficiently replicate acute mastitis for bacterial evaluations. Low and high-concentration groups were designed to observe the bactericidal effect of cefquinome on *S. agalactiae*. The low-concentration group achieved bactericidal efficacy when the drug concentration was >4 × MIC. However, for the high-concentration group, cefquinome achieved only a bacteriostatic effect. These data agree with a previous report [39]. Significant differences were observed between the low-concentration and high-concentration groups ($p<0.05$) that
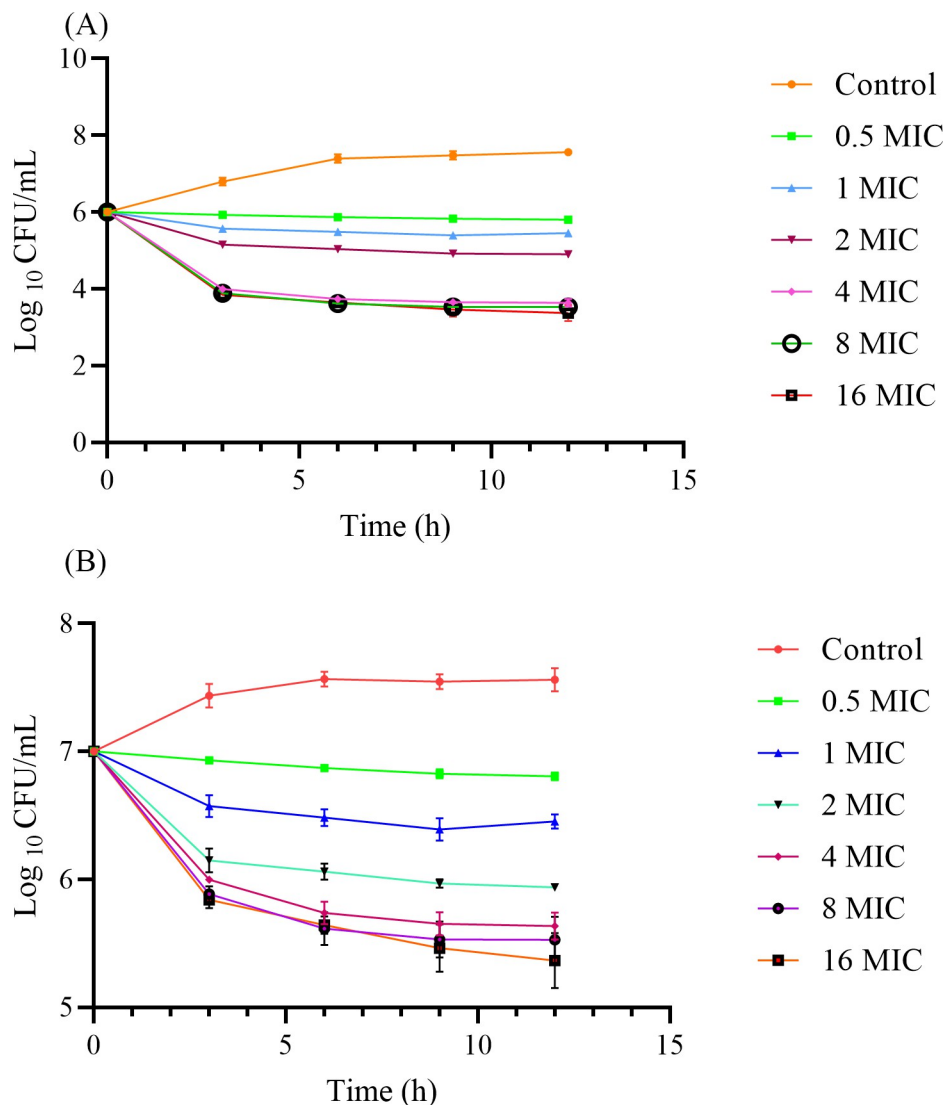
Fig 3. *In vitro* cefquinome killing curve against *S. agalactiae* 3–64. (A) Antibacterial effects begin at an initial inoculum of 10^6 CFU/mL. (B) Antibacterial effects begin at an initial inoculum of 10^7 CFU/mL. The bacterial population was measured at 0, 3, 6, 9, and 12 hrs by counting visible bacterial colonies.

https://doi.org/10.1371/journal.pone.0278306.g003

may be related to the fact that cefquinome is a beta-lactam which is a bactericidal drug at the exponentialstage of bacteria.

Penicillin-binding proteins (PBPs) are needed for the survival, growth, and reproduction of bacteria. PBPs are also the binding sites for beta-lactam antibiotics [40] which cause bacterial death by creating defects in bacterial cell walls [41]. In this study, based on the bacterial killing curves, the low-concentration group had a higher growth rate (more bacteria were present at the exponential stage) compared to the high-concentration group. The greater number of exponential growing bacteria means that more PBPs could combine with the cefquinome. Hence, the bactericidal effect in the low-concentration group was greater than that in the high-concentration group.

Different bacteria have been used to describe the association between PK/PD indexes and cefquinome antibacterial activity in different animal infection models. A prior report used
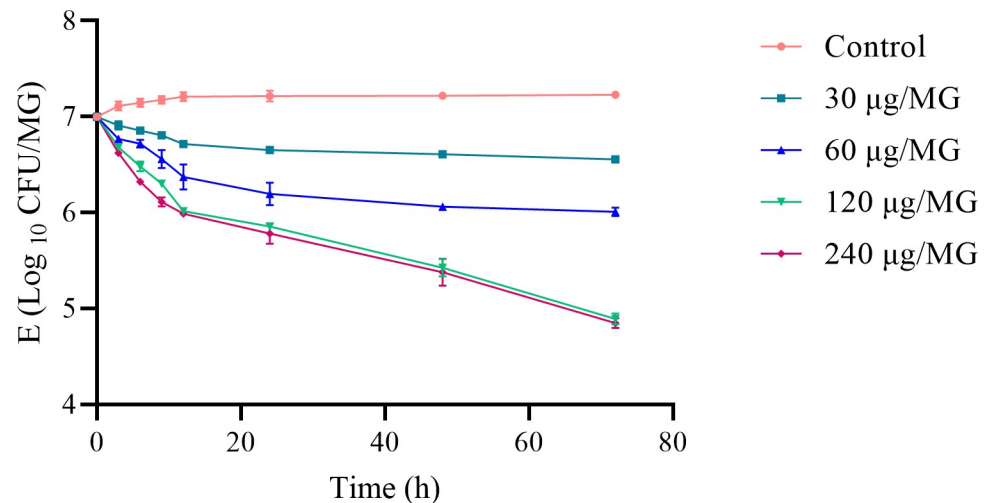
Fig 4. *In vivo* cefquinome PD studies in a murine mastitis model. The change in the $\log_{10}$ CFU/MG was measured after 72 hrs of treatment. Changes in the viable cell density (CFU/MG) of *S. agalactiae* and the concentrations of antibiotics (×MIC) *in vivo* following a single treatment with cefquinome. Test dosage regimens were a single dose of 30 μg/MG, 60 μg/MG, 120 μg/MG, and 240 μg/MG by intramammary administration, (n = 4 for mice, and 8 mammary glands). The bacterial population was measured by counting visible bacterial colonies.

https://doi.org/10.1371/journal.pone.0278306.g004

Haemophilus parasuis to study the antibacterial activity of cefquinome. The data suggested that the %T > MIC required for 3-$\log_{10}$ drop and 4-$\log_{10}$ drop were 61% and 71%, respectively [42]. A later study investigated the effects of cefquinome on *Actinobacillus pleuropneumoniae* using a piglet tissue cage model and reported that %T > MIC achieved 11.59%, 27.49%, and 59.81% with respective 1/3-$\log_{10}$, 2/3-$\log_{10}$, and 1-$\log_{10}$ reductions [43]. The same group also used *Escherichia coli* to examine cefquinome antibacterial efficacy and calculated that the values of %T > MIC to achieve 1/6-$\log_{10}$ reductions, 1/3-$\log_{10}$ reductions, and 1/2-$\log_{10}$ reductions were 3.97%, 17.08%, and 52.68%, respectively [44]. The efficacy of cefquinome was also reported for *Klebsiella pneumonia* and *Staphylococcus aureus* in an *ex vivo* dog model and an *in vivo* rabbit tissue cage infection model [21, 45]. All these studies demonstrated that
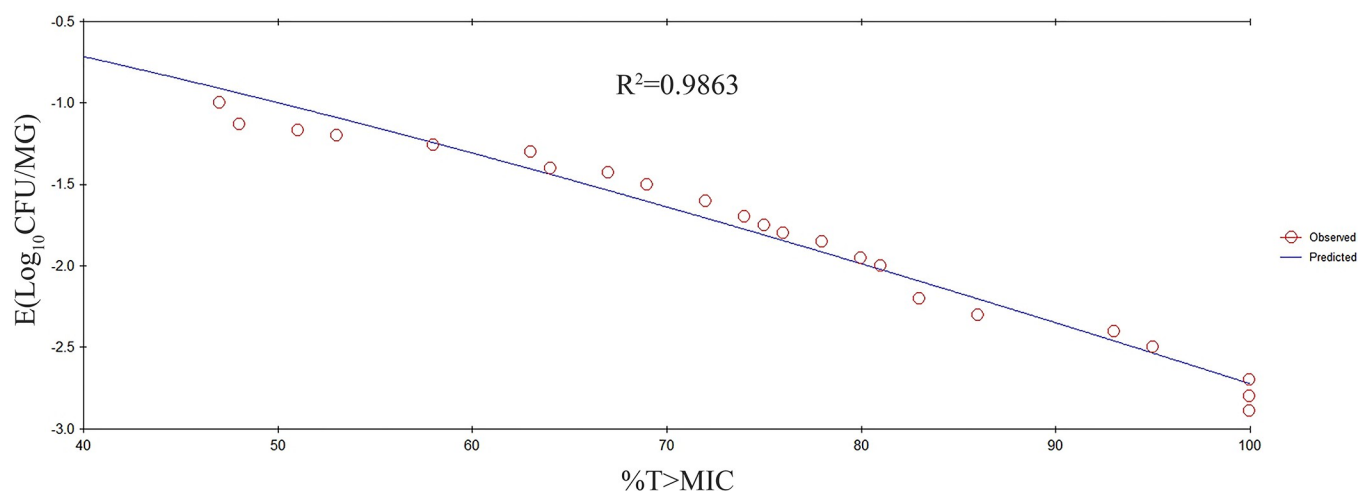

Fig 5. The inhibitory Sigmoid E_{max} relationship between *in vivo* antibacterial effects (△log CFU/MG) and PK/PD index of %T>MIC against *S. agalactiae* 3–64. The line represents the fit of the model to the data. The circles represent the observed PD data. R^2 indicates the correlation coefficient.

https://doi.org/10.1371/journal.pone.0278306.g005

Fig 6. The inhibitory Sigmoid E_{max} relationship between *in vivo* antibacterial effects ($\triangle$log CFU/MG) and the PK/PD index of AUC/MIC against *S. agalactiae* 3–64. The line represents the fit of the model to the data. The circles represent the observed PD data. R^2 indicates the correlation coefficient.
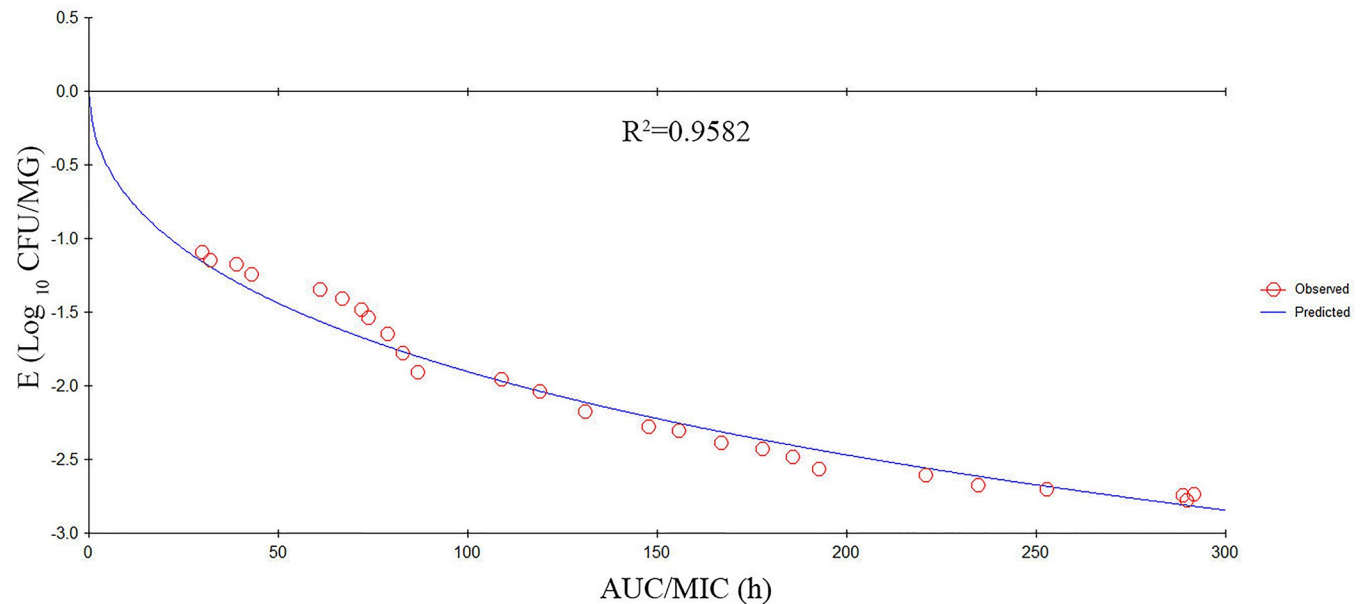
cefquinome had effective antimicrobial activity against these pathogens. However, to the best of our knowledge, no previous study has reported on the efficacy of cefquinome against *S. agalactiae*.

In the current study, we used an experimental *S. agalactiae* mastitis model system to investigate the interactions between the PK/PD indexes and cefquinome activity against *S. agalactiae*. The %T>MIC was the PK/PD index that most effectively described the antibacterial activity of cefquinome against *S. agalactiae*. When the *in vivo* %T > MIC values were 31%, 47%, and 81%, there were 0.5-$\log_{10}$ units, 1-$\log_{10}$ units, 2-$\log_{10}$ units reductions observed, respectively. Studies have shown that %T > MIC is a vital index for describing the PK/PD relationship of the cefquinome concerning bactericidal activity [46, 47]. Here, the correlation coefficient (R^2)
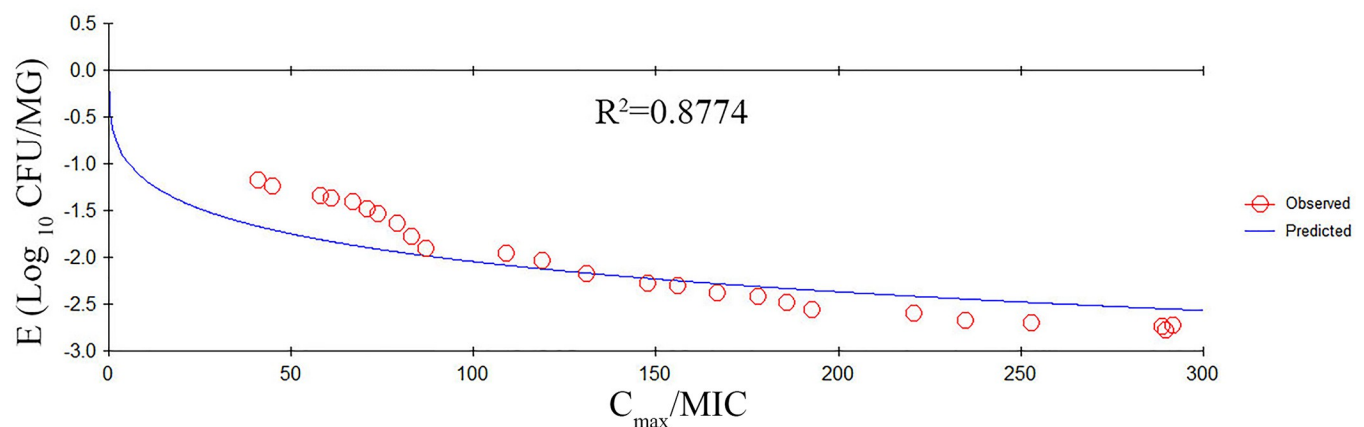

Fig 7. The inhibitory Sigmoid E_{max} relationship between *in vivo* antibacterial effects ($\triangle$log CFU/MG) and the PK/PD index of C_{max}/MIC against *S. agalactiae* 3–64. The line represents the fit of the model to the data. The circles represent the observed PD data. R^2 indicates the correlation coefficient.

Table 3. The key PK/PD parameters for %T>MIC to achieve different antibacterial effects.

Parameter	Values
E_{max} (log$_{10}$CFU/MG)	1.12
E_0 (log$_{10}$ CFU/MG)	-2.89
EC_{50} (h)	44.79
N	3.26
%T>MIC for 0.5-log$_{10}$ reduction	31
%T>MIC for 1-log$_{10}$ reduction	47
%T>MIC for 2-log$_{10}$ reduction	81

E_{max} represents the $\triangle$logCFU72 h in the drug-free control samples; E_0 indicates the $\triangle$logCFU72 h in experimental samples containing cefquinome when reached the maximum antibacterial effect; EC_{50} denotes the PK-PD indexes for the drug that means 50% of the maximum antibacterial effect, and N indicates the Hill coefficient (indicating effect curve steepness estimates for PK-PD indexes).

https://doi.org/10.1371/journal.pone.0278306.t003

values of $\%T > MIC$, AUC/MIC, and C_{max}/MIC were 0.9863, 0.9582, and 0.8774, respectively. AUC/MIC has been used to describe the relationship between PK and PD for concentration-dependent drugs. However, in this study, the R^2 of $\%T > MIC$ and AUC/MIC were very close showing that both indexes were useful in this model. These data are in agreement with a previous report by Yu et al. [28]. The cefquinome concentrations in the blood and MG were not identical due to the blood-milk barrier which explains this result.

In this study, we showed that specific doses of cefquinome cause different therapeutic impacts on the *S. agalactiae*-induced mastitis model. We also demonstrated that cefquinome can cause a reduction of 2.8-log$_{10}$ CFU/MG in the *in vivo* killing-time curve to achieve a bactericidal effect *in vivo*.

Supporting information

S1 Fig. Chromatograms of blank plasma sample, standard cefquinome solution sample and sample solution sample. Together with standard curve. The samples were detected by LC-ESI-MS/MS as described in the method section.
(TIF)

S1 Table. *In vitro* cefquinome killing curve against *S. agalactiae* 3–64. Antibacterial effects begin at an initial inoculum of 10^6 CFU/mL.
(DOC)

S2 Table. *In vitro* cefquinome killing curve against *S. agalactiae* 3–64. Antibacterial effects begin at an initial inoculum of 10^7 CFU/mL.
(DOC)

S3 Table. *In vivo* cefquinome PD studies in a murine mastitis model. Testing dosage regimens were a single dose of 30 μg/MG, 60 μg/MG, 120 μg/MG, and 240 μg/MG by intramammary administration.
(DOCX)

S4 Table. I*n vivo* antibacterial effects ($\triangle$log CFU/MG) *versus* PK/PD index of %T>MIC against *S. agalactiae* 3–64.
(DOC)

S5 Table. I*n vivo* antibacterial effects (△log CFU/MG) *versus* PK/PD index of AUC/MIC against *S. agalactiae* 3–64.
(DOCX)

S6 Table. I*n vivo* antibacterial effects (△log CFU/MG) *versus* PK/PD index of C_{max}/MIC against *S. agalactiae* 3–64.
(DOC)

Acknowledgments

The authors are grateful to all participating dairy farms and Dr. Chuanshi Zhang from Chongqing Three Gorges Vocational College for helpful discussion regarding the PK/PD index.

Author Contributions

Conceptualization: Yun Liu.

Formal analysis: Kang Yong, Qian Lv, Yi Zhang.

Investigation: Qingwen Yang, Chenghuan Zhang, Xuesong Liu.

Methodology: Qingwen Yang, Chenghuan Zhang, Xuesong Liu, Longfei Zhang.

Resources: Liang Chen, Peng Zhong, Yun Liu.

Software: Xuesong Liu.

Writing – original draft: Qingwen Yang.

Writing – review & editing: Yun Liu.

References

1. Bradley A. Bovine mastitis: an evolving disease. Veterinary Journal. 2002; 164(2): 116–128. https://doi.org/10.1053/tvjl.2002.0724 PMID: 12359466

2. Zhao X, Lacasse P. Mammary tissue damage during bovine mastitis: causes and control. Journal of Animal Scicience. 2008; 86(13 Suppl): 57–65. https://doi.org/10.2527/jas.2007-0302 PMID: 17785603

3. Ruegg PL. A 100-Year Review: Mastitis detection, management, and prevention. Journal of Dairy Science. 2017; 100(12): 10381–10397. https://doi.org/10.3168/jds.2017-13023 PMID: 29153171

4. Jain NC. Common mammary pathogens and factors in infection and mastitis. Journal of Dairy Science. 1979; 62(1): 128–134. https://doi.org/10.3168/jds.S0022-0302(79)83214-2 PMID: 572381

5. Keefe GP. *Streptococcus agalactiae* mastitis: a review. The Canadian Veterinary Journal. 1997; 38(7): 429–437. PMID: 9220132

6. Marshal MM, Søren SN, Tariq H, Toft N. Spatiotemporal patterns, annual baseline and movement-related incidence of *Streptococcus agalactiae* infection in Danish dairy herds: 2000–2009. Preventive veterinary medicine. 2014; 113(2): 219–230. https://doi.org/10.1016/j.prevetmed.2013.10.020 PMID: 24269038

7. Keefe GP, Dohoo IR, Spangler E. Herd prevalence and incidence of *Streptococcus agalactiae* in the dairy industry of Prince Edward Island. Journal of Dairy Science. 1997; 80(3):464–470. https://doi.org/10.3168/jds.S0022-0302(97)75958-7 PMID: 9098795

8. Lin LS, Huang XJ, Yang HF, He YX, He XF, Huang JH, et al. Molecular epidemiology, antimicrobial activity, and virulence gene clustering of *Streptococcus agalactiae* isolated from dairy cattle with mastitis in China. Journal of Dairy Science. 2021; 104(4): 4893–4903. https://doi.org/10.3168/jds.2020-19139 PMID: 33551160

9. Han GL, Zhang BH, Luo ZD, Lu B, Luo ZZ, Zhang JR, et al. Molecular typing and prevalence of antibiotic resisitance and virulence genes in *Streptococcus agalactiae* isolated from Chinese dairy cows with clinical mastitis. PLoS One. 2022; 17(5): e0268262. https://doi.org/10.1371/journal.pone.0268262 PMID: 35522690

10. Bi YL, Wang YJ, Qin Y, Vallverdú RJ, Maldonado GJ, Sun W, et al. Prevaence of bovine mastitis pathogens in bulk tank milk in China. PLoS One. 2016; 11(5): e0155621. https://doi.org/10.1371/journal.pone.0155621 PMID: 27187065

11. Tian XY, Zheng N, Han RW, Ho H, Wang J, Wang YT, et al. Antimicrobial resistance and virulence genes of *Streptococcus* isolated from dairy cows with mastitis in China. Microbial Pathogenesis. 2019; 131: 33–39. https://doi.org/10.1016/j.micpath.2019.03.035 PMID: 30940606

12. Ding YX, Zhao JL, He XL, Li M, Guan H, Zhang ZY, et al. Antimicrobial resistance and virulence-related genes of *Streptococcus* obtained from dairy cows with mastitis in Inner Mongolia, China. Pharmaceutical Biology. 2016; 54(1): 162–167. https://doi.org/10.3109/13880209.2015.1025290 PMID: 25856704

13. Brouillette E, Malouin F. The pathogenesis and control of S*taphylococcus aureus*-induced mastitis: Study models in the mouse. Microbes and Infection. 2005; 7(3): 560–568. https://doi.org/10.1016/j.micinf.2004.11.008 PMID: 15777742

14. Chandler RL. Experimental bacterial mastitis in the mouse. Journal of Medical Microbiology. 1970; 3 (2):273–282. https://doi.org/10.1099/00222615-3-2-273 PMID: 4989101

15. Notebaert S, Demon D, Berghe TV, Vandenabeele P, Meyer E. Inflammatory mediators in *Escherichia coli*-induced mastitis in mice. Comparative Immunology, microbiology and infectious diseases. 2008; 31(6): 551–565. https://doi.org/10.1016/j.cimid.2007.10.004 PMID: 18243314

16. Geng HJ, Zou W, Zhang MX, Xu L, Liu FM, Li XY, et al. Evaluation of phage therapy in the treatment of *Staphylococcus aureus*-induced mastitis in mice. Folia Microbiologica. 2020; 65(2): 339–351. https://doi.org/10.1007/s12223-019-00729-9 PMID: 31256341

17. Chinchali JF, Kaliwal BB. Histopathology of mammary gland in *Staphylococcus aureus* induced mastitis in mice. Asian Pacific Journal of Tropical Disease. 2014; 4(Suppl 1): S320–S325. https://doi.org/10.1016/S2222-1808(14)60463-1

18. Limbert M, Isert D, Klesel N, Markus A, Seeger K, Seibert G et al. Antibacterial activities in vitro and in vivo and pharmacokinetics of cefquinome (HR 111V), a new broad-spectrum cephalosporin. Antimicrobial Agents and Chemotherapy. 1991; 35(1): 14–19. https://doi.org/10.1128/AAC.35.1.14 PMID: 2014969

19. Swinkels JM, Lam TJGM, Green MJ, Bradley AJ. Effect of extended cefquinome treatment on clinical persistence or recurrence of environmental clinical mastitis. Veterinary Journal. 2013; 197(3): 682–687. https://doi.org/10.1016/j.tvjl.2013.03.010 PMID: 23702283

20. Taverne FJ, Geijlswijk IMV, Heederik DJJ, Wagenaar JA, Mouton JW. Modelling concentrations of antimicrobial drugs: comparative pharmacokinetics of cephalosporin antimicrobials and accuracy of allometric scaling in food-producing and companion animals. BMC Veterinary Research. 2016; 12(1): 185. https://doi.org/10.1186/s12917-016-0817-2 PMID: 27596044

21. Xiong MP, Wu X, Ye XM, Zhang LF, Zeng SY, Huang ZL, et al. Relationship between cefquinome PK/PD parameters and emergence of resistance of *Staphylococcus aureus* in rabbit tissue-cage infection model. Frontiers in Microbiology. 2016; 7: 874. https://doi.org/10.3389/fmicb.2016.00874 PMID: 27375594

22. Shpigel NY, Levin D, Winkler M, Saran A, Ziv G, Böttner A. Efficacy of cefquinome for treatment of cows with mastitis experimentally induced using *Escherichia coli*. Journal of Dairy Science. 1997; 80 (2): 318–323. https://doi.org/10.3168/jds.S0022-0302(97)75941-1 PMID: 9058274

23. National Research Council. Guide for the care and use of laboratory animals. Washington, DC: National Academy Press; 1996.

24. CLSI, editor. Performance Standards for antimicrobial disk and dilution susceptibility tests for bacteria isolated from animals; approved standard, 4th ed. CLSI document VET01. Wayne; Clinical and Laboratory Standards Institute; 2013.

25. Balaje RM, Sidhu PK, Kaur G, Rampal S. Mutant prevention concentration and PK-PD relationships of enrofloxacin for *Pasteurella multocida* in buffalo calves. Research in Veterinary Science. 2013; 95(3): 1114–1124. https://doi.org/10.1016/j.rvsc.2013.07.019 PMID: 23941961

26. Ramalingam B, Sidhu PK, Kaur G, Venkatachalam D, Rampal S. Mutant prevention concentration, pharmacokinetic-pharmacodynamic integration, and modeling of enrofloxacin data established in diseased buffalo calves. Journal of Veterinary Pharmacology and Therapeutics. 2015; 38(6): 529–536. https://doi.org/10.1111/jvp.12223 PMID: 25776301

27. Zhao DH, Wang XF, Wang Q, Li LD. Pharmacokinetics, bioavailability and dose assessment of cefquinome against *Escherichia coli* in black swans (*Cygnus atratus*). BMC Veterinary Research. 2017; 13 (1): 226. https://doi.org/10.1186/s12917-017-1148-7 PMID: 28754112

28. Yu Y, Zhou YF, Chen MR, Li X, Qiao GL, Sun J, et al. In vivo pharmacokinetics/pharmacodynamics of cefquinome in an experimental mouse model of *Staphylococcus aureus* mastitis following intramammary infusion. PLoS One. 2016; 11(5): e0156273. https://doi.org/10.1371/journal.pone.0156273 PMID: 27218674

29. Yu Y, Fang JT, Sun J, Zheng M, Zhang Q, He JS, et al. Efficacy of cefquinome against *Escherichia coli* environmental mastitis assessed by pharmacokinetic and pharmacodynamic integration in lactating mouse model. Frontiers in Microbiology. 2017; 8: 1445. https://doi.org/10.3389/fmicb.2017.01445 PMID: 28824576

30. Zeng DP, Sun MZ, Lin ZM, Li M, Gehring R, Zeng ZL. Pharmacokinetics and pharmacodynamics of tildipirosin against *Pasteurella multocida* in a murine lung infection model. Frontiers in Microbiology. 2018; 9: 1038. https://doi.org/10.3389/fmicb.2018.01038 PMID: 29867911

31. Wang JY, Hao HH, Huang LL, Liu ZL, Chen DM, Yuan ZH. Pharmacokinetic and pharmacodynamic integrtion and modeling of enrofloxacin in swine for *Escherichia coli*. Frontiers in Microbiology. 2016; 7: 36. https://doi.org/10.3389/fmicb.2016.00036 PMID: 26870006

32. Wang HL, Chen C, Chen XJ, Zhang JJ, Liu YM, Li XB. PK/PD modeling to assess rifaximin clinical dosage in a mouse model of *Staphylococcus aureus*-induced mastitis. Frontiers in Veterinary Science. 2021; 8:651369. https://doi.org/10.3389/fvets.2021.651369 PMID: 34195244

33. Liu XS, Yang QW, FAN YY, Du YY, Lei L, Wang D et al. Pharmacokinetic and pharmacodynamics of enrofloxacin treatment of *Escherichia coli* in a murine thigh infection modeling. BMC Veterinary Research. 2021; 17(1): 212. https://doi.org/10.1186/s12917-021-02908-8 PMID: 34107961

34. Jing W, Shan Q, Ding HZ, Liang CP, Zeng ZL. Pharmacodynamics of cefquinome in a neutropenic mouse thigh model of *Staphylococcus aureus* infection. Antimicrobial Agents and Chemotherapy. 2014; 58(6): 3008–3012. https://doi.org/10.1128/AAC.01666-13 PMID: 24614373

35. Toutain PL, Lees P. Integration and modelling of pharmacokinetic and pharmacodynamic data to optimize dosage regimens in veterinary medicine. Journal of Veterinary Pharmacology Therapeutics. 2004; 27(6): 467–477. https://doi.org/10.1111/j.1365-2885.2004.00613.x PMID: 15601441

36. Yu Y, Zhou YF, Li X, Chen MR, Qiao GL, Sun J, et al. Dose assessment of cefquinome by pharmacokinetic/pharmacodynamic modeling in mouse model of *Staphylococcus aureus* mastitis. Frontiers in Microbiology. 2016; 7: 1595. https://doi.org/10.3389/fmicb.2016.01595 PMID: 27774090

37. Li YF, Wang L, Gu XY, Zeng ZL, He LM, Yang F, et al. Pharmacokinetics and residues of cefquinome in milk of lactating Chinese dairy cows after intramammary administration. Journal of Integrative Agriccullture. 2014; 13(12): 2750–2757. https://doi.org/10.1016/S2095-3119(14)60757-7

38. CVMP (Commimitte for Veterinary Medical Products). Cefquinome Summary Report. 1999; 545.

39. Guo CN, Liao XP, Wang MR, Wang F, Yan CQ, Xiao X, et al. In vivo pharmacodynamics of cefquinome in a neutropenic mouse thigh model of *Streptococcus suis* serotype 2 at varied initial inoculum sizes. Antimicrobial Agents and Chemotherapy. 2015; 60(2): 1114–1120. https://doi.org/10.1128/AAC.02065-15 PMID: 26666923

40. Buynak JD. Understanding the longevity of the beta-lactam antibiotics and of antibiotic/beta-lactamase inhibitor combinations. Biochemical Pharmacology. 2006; 71(7): 930–940. https://doi.org/10.1016/j.bcp.2005.11.012 PMID: 16359643

41. Satta G, Cornaglia G, Mazzariol A, Golini G, Valisena S, Fontana R. Target for bacteriostatic and bactericidal activities of beta-lactam antibiotics against *Escherichia coli* resides in different penicillin-binding proteins. Antimicrobial Agents and Chemotherapy. 1995; 39(4): 812–818. https://doi.org/10.1128/aac.39.4.812 PMID: 7785976

42. Xiao X, Sun J, Huang RJ, Huang T, Qiao GG, Zhou YF, et al. In vitro dynamic pharmacokinetic/pharmacodynamic (PK/PD) modeling and PK/PD cutoff of cefquinome against *Haemophilus parasuis*. BMC Veterinary Research. 2015; 11: 33. https://doi.org/10.1186/s12917-015-0343-7 PMID: 25889187

43. Zhang LF, Wu X, Huang ZL, Zhang N, Wu YZ, Cai QR, et al. Pharmacokinetic/pharmacodynamic assessment of cefquinome against *Actinobacillus Pleuropneumoniae* in a piglet tissue cage infection model. Veterinary Microbiology. 2018; 219: 100–106. https://doi.org/10.1016/j.vetmic.2018.02.027 PMID: 29778180

44. Gu MX, Zhang N, Zhang LF, Xiong MP, Yang YY, Gu XY, et al. Response of a clinical *Escherichia coli* strain to repeated cefquinome exposure in a piglet tissue-cage model. BMC Veterinary Research. 2015; 11: 169. https://doi.org/10.1186/s12917-015-0486-6 PMID: 26209108

45. Zhang B, Gu X, Li X, Zhang N, Shen X, Ding H. Pharmacokinetics and ex-vivo pharmacodynamics of cefquinome against *Klebsiella pneumonia* in healthy dogs. Journal Veterinary Pharmacology Therapeutics. 2014; 37(4): 367–373. https://doi.org/10.1111/jvp.12100 PMID: 24372291

46. Shan Q, Liang CP, Wang J, Li JF, Zeng ZL. In vivo activity of cefquinome against *Escherichia coli* in the thighs of neutropenic mice. Antimicrobial Agents and Chemotherapy. 2014; 58(10): 5943–5949. https://doi.org/10.1128/AAC.03446-14 PMID: 25070101

47. Ahmad I, Huang LL, Hao HH, Sanders P, Yuan ZH. Application of PK/PD modeling in veterinary field: dose optimization and drug resistance prediction. BioMed Research International. 2016; 2016: 5465678. https://doi.org/10.1155/2016/5465678 PMID: 26989688